Rhenium(I) Tricarbonyl Complexes with New Pyridine Ligands Containing Crown Ether-Annelated or Anthracene-Functionalized 1,3-Dithiole-2-ylidene

Wei Liu, Ya Chen, Ru Wang, Xin-Hui Zhou, Jing-Lin Zuo,* and Xiao-Zeng You

Coordination Chemistry Institute and the State Key Laboratory of Coordination Chemistry, School of Chemistry and Chemical Engineering, Nanjing University, Nanjing 210093, People's Republic of China

Received February 26, 2008

Two bispyridine ligands containing crown ether-annelated or anthryl-substituted 1,3-dithiole-2-ylidene, 4,5-dithia-(3′,6′,9′,12′-tetraoxatetradecyl)-2-bis(2-pyridyl)methylene-1,3-dithiole (BPyDT(O_4S_2), **3**) and 4-methylthio-5-[{2-(9′-anthryloxy)-ethyl}thio]-2-bis(2-pyridyl)methylene-1,3-dithiole (BPyDT(SMe)(SEA), **7**), have been synthesized and characterized. The rhenium(I) tricarbonyl complexes $ClRe(CO)_3$-(BPyDT(O_4S_2)) (**4**) and $BrRe(CO)_3$(BPyDT(SMe)(SEA)) (**8**) have been prepared based on them. The crystal structures of compounds **3**, **4**, and **8** have been determined. Complexes **4** and **8** exhibit greenish-yellow emission, while ligands **3** and **7** show blue luminescence in fluid solutions at room temperature. Redox properties of **3**, **4**, **7**, and **8** have been investigated by cyclic voltammetry, and the crown ether-annelated compounds **3** and **4** show significant Na^+-binding properties with large positive redox shifts.

Introduction

Luminescent polypyridine complexes with d^6 electronic configuration transition metals have attracted intense interest in recent years, as they are employed for biological labeling and probes,[1,2] as well as photosensitizers for solar energy conversion,[3] and electron transfer reactions.[4] Among them, rhenium(I) tricarbonyl complexes containing bis- or polypyridine-type ligands are widely studied, not only for their synthesis facility and chemical stability but also for their excellent photophysical and photochemical properties.[5]

Compounds with a 1,3-dithiole-2-ylidene moiety usually have a delocalized electron system and can be switched reversibly in different oxidation states.[6] Studies on these redox-active molecular systems have progressed substantially. We have been particularly interested in this field for their electron-delocalized character and synthetic transformation facility, which are crucial for developing and fabricating novel advanced materials.[7] However, to the best of our knowledge, little attention has been focused on the combination of multi-sulfur systems and rhenium(I) bispyridine-type complexes. To investigate the effect of such a combination, we have recently reported the synthesis

Chart 1

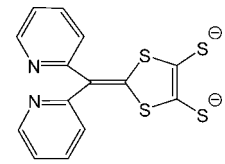

$BPyDTS_2$

* To whom correspondence should be addressed. E-mail: zuojl@nju.edu.cn. Fax: +86-25-83314502.

(1) (a) Yam, V. W. W.; Wong, K. M. C.; Lee, V. W. M.; Lo, K. K. W.; Cheung, K. K. *Organometallics* **1995**, *14*, 4034. (b) Beer, P. D.; Dent, S. W. *Chem. Commun.* **1998**, 825. (c) Beer, P. D.; Timoshenko, V.; Maestri, M.; Passaniti, P.; Balzani, V. *Chem. Commun.* **1999**, 1755. (d) Di Bilio, A. J.; Crane, B. R.; Wehbi, W. A.; Kiser, C. N.; Abu-Omar, M. M.; Carlos, R. M.; Richards, J. H.; Winkler, J. R.; Gray, H. B. *J. Am. Chem. Soc.* **2001**, *123*, 3181. (e) Lo, K. K. W.; Hui, W. K.; Ng, D. C. M.; Cheung, K. K. *Inorg. Chem.* **2002**, *41*, 40. (f) Uppadine, L. H.; Keene, F. R.; Beer, P. D. *J. Chem. Soc., Dalton Trans.* **2001**, 2188. (g) Sun, S. S.; Lees, A. J.; Zavalij, P. Y. *Inorg. Chem.* **2003**, *42*, 3445. (h) Lazarides, T.; Miller, T. A.; Jeffery, J. C.; Ronson, T. K.; Adams, H.; Ward, M. D. *J. Chem. Soc., Dalton Trans.* **2005**, 528.

(2) (a) MacQueen, D. B.; Schanze, K. S. *J. Am. Chem. Soc.* **1991**, *113*, 6108. (b) Yoon, D. I.; Berg-Brennan, C. A.; Lu, H.; Hupp, J. T. *Inorg. Chem.* **1992**, *31*, 3192. (c) Shen, Y.; Sullivan, B. P. *Inorg. Chem.* **1995**, *34*, 6235. (d) Wong, K. M. C.; Li, W. P.; Cheung, K. K.; Yam, V. W. W. *New J. Chem.* **2005**, *29*, 165. (e) Lo, K. K. W.; Tsang, K. H. K.; Zhu, N. *Organometallics* **2006**, *25*, 3220. (f) Lewis, J. D.; Clark, I. P.; Moore, J. N. *J. Phys. Chem. A* **2007**, *111*, 50.

(3) (a) Caspar, J. V.; Sullivan, B. P.; Meyer, T. J. *Inorg. Chem.* **1984**, *23*, 2098. (b) Kober, E. M.; Marshall, J. L.; Dressick, W. J.; Sullivan, B. P.; Meyer, T. J. *Inorg. Chem.* **1985**, *24*, 2755. (c) Meyer, T. J. *Pure Appl. Chem.* **1986**, *58*, 1193. (d) Wrighton, M. S.; Geoffroy, G. L. *Organometallic Photochemistry*; Academic Press: New York, 1979; Chapter 2. (e) Della Ciana, L.; Dressicak, W. J.; Sandrini, D.; Maestri, M.; Ciano, M. *Inorg. Chem.* **1990**, *29*, 2792. (f) Nazeeruddin, M. K.; Klein, C.; Liska, P.; Grätzel, M. *Coord. Chem. Rev.* **2005**, *249*, 1460. (g) Polo, A. S.; Itokazu, M. K.; Frin, K. M.; Patrocínio, A. O. de T.; Iha, N. Y. M. *Coord. Chem. Rev.* **2006**, *250*, 1669, and references therein.

(4) Reece, S. Y.; Nocera, D. G. *J. Am. Chem. Soc.* **2005**, *127*, 9448.

(5) See for examples:(a) Wrighton, M.; Morse, D. L. *J. Am. Chem. Soc.* **1974**, *96*, 998. (b) Lucia, L. A.; Abboud, K.; Schanze, K. S. *Inorg. Chem.* **1997**, *36*, 6224. (c) Stufkens, D. J.; Vlček, A., Jr. *Coord. Chem. Rev.* **1998**, *177*, 127. (d) Tapolsky, G.; Duesing, R.; Meyer, T. J. *Inorg. Chem.* **1990**, *29*, 2285. (e) Wallace, L.; Woods, C.; Rillema, D. P. *Inorg. Chem.* **1995**, *34*, 2875. (f) Yam, V. W. W.; Lau, V. C. Y.; Cheung, K. K. *J. Chem. Soc., Chem. Commun.* **1995**, 259. (g) Yam, V. W. W.; Lo, W. Y.; Lam, C. H.; Fung, W. K. M.; Wong, K. M. C.; Lau, V. C. Y.; Zhu, N. *Coord. Chem. Rev.* **2003**, *245*, 39. (h) Gabrielsson, A.; Hartl, F.; Zhang, H.; Lindsay Smith, J. R.; Towrie, M.; Vlček, A., Jr.; Perutz, R. N. *J. Am. Chem. Soc.* **2006**, *128*, 4253. (i) Berger, S.; Klein, A.; Kaim, W.; Fiedler, J. *Inorg. Chem.* **1998**, *37*, 5664.

(6) See for examples:(a) Segura, J.; Martín, N. *Angew. Chem., Int. Ed.* **2001**, *40*, 1372. (b) Bryce, M. R.; Batsanov, A. S.; Finn, T.; Hansen, T. K.; Howard, J. A. K.; Kamenjicki, M.; Lednev, I. K.; Asher, S. A. *Chem. Commun.* **2000**, 295. (c) Christensen, C. A.; Batsanov, A. S.; Bryce, M. R. *J. Am. Chem. Soc.* **2006**, *128*, 10484. (d) Baudron, S. A.; Hosseini, M. W. *Inorg. Chem.* **2006**, *45*, 5260. (e) Wu, H.; Zhang, D.; Su, L.; Ohkubo, K.; Zhang, C.; Yin, S.; Mao, L.; Shuai, Z.; Fukuzumi, S.; Zhu, D. *J. Am. Chem. Soc.* **2006**, *129*, 6839. (f) Gavrilenko, K. S.; Le Gal, Y.; Cador, O.; Golhen, S.; Ouahab, L. *Chem. Commun.* **2007**, 280.

(7) (a) Ji, Y.; Zhang, R.; Li, Y. J.; Li, Y. Z.; Zuo, J. L.; You, X. Z. *Inorg. Chem.* **2007**, *46*, 866. (b) Wen, H. R.; Li, C. H.; Song, Y.; Zuo, J. L.; Zhang, B.; You, X. Z. *Inorg. Chem.* **2007**, *46*, 6837. (c) Liu, W.; Lu, J. H.; Ji, Y.; Zuo, J. L.; You, X. Z. *Tetrahedron Lett.* **2006**, *47*, 3431.

10.1021/om800178k CCC: $40.75
Publication on Web 05/23/2008

Scheme 1. Synthetic Routes to Ligand 3 and Complex 4[a]

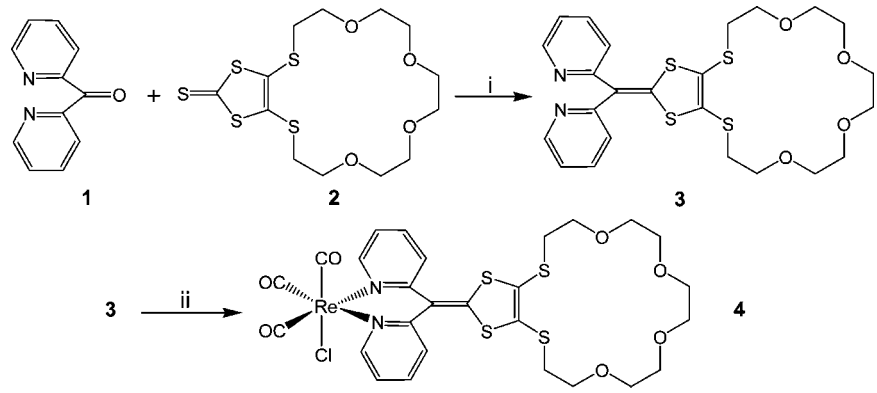

[a] (i) $P(OEt)_3$, reflux; (ii) $Re(CO)_5Cl$, toluene.

and photophysical properties of two tricarbonyl rhenium(I) heteronuclear complexes bridged by the bispyridine ligand $BPyDTS_2$ (Chart 1).[8] Interestingly, this deprotected ligand also offers feasibility to be modified by introducing selected functional groups at peripheral sites. It is anticipated that multifunctional properties and cooperative behavior could be achieved through modification. O, S mixed crown ether units with different ring size are well-known building blocks and being explored for binding alkali metal ion selectively.[9,10] The anthracene moiety, as a classic luminophore, is employed as a tecton for designing and constructing photonic devices.[11]

We report herein two new rhenium(I) complexes, $ClRe(CO)_3(BPyDT(O_4S_2))$ (**4**) and $BrRe(CO)_3(BPyDT(SMe)(SEA))$ (**8**), in which the pyridine ligands consist of coupled bis(2-pyridyl) and extended 1,3-dithiole-2-ylidene. The 1,3-dithiole-2-ylidene moieties are functionalized by an annelated crown ether in **4** and an ethyloxy-linked anthracene in **8**. The preparation, spectroscopy, redox properties, and structural analyses of these compounds are described. In particular, the cation-binding properties of crown-incorporated complex **4** and its precursor ligand **3** have been thoroughly investigated.

Scheme 2. Synthetic Routes to Ligand 7 and Complex 8[a]

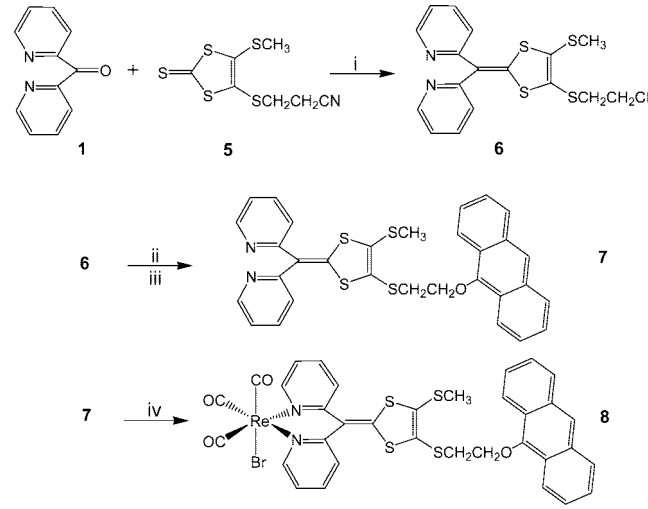

[a] (i) $P(OEt)_3$, toluene; (ii) $CsOH \cdot H_2O$; (iii) 9-(2-bromoethoxy)anthracene; (iv) $Re(CO)_5Br$, toluene.

Experimental Section

General Considerations. Schlenk techniques were used in carrying out manipulations under a N_2 atmosphere. The IR spectra were taken on a Vector22 Bruker spectrophotometer (400−4000 cm^{-1}) with KBr pellets. Absorption spectra were measured on a UV-3100 spectrophotometer. Elemental analyses for C, H, and N were performed on a Perkin-Elmer 240C analyzer. Emission measurements were carried out on an Aminco Bowman Series 2 luminescence spectrometer in a 1 cm quartz cell. NMR spectra were measured on a Bruker AM 500 spectrometer. Melting points were determined with an X-4 digital micro melting point apparatus and uncorrected. Cyclic voltammetry was performed on a CHI660b electrochemical analytical instrument, with platinum as the working and counter electrodes, Ag/Ag^+ as the reference electrode, and 0.1 M n-Bu_4NClO_4 as the supporting electrolyte. Mass spectra were recorded on a Bruker Autoflex ^{II}TM instrument for MALDI-TOF-MS or on a Varian MAT 311A instrument for ESI-MS. The compounds 5,8,11,14-tetraoxa-2,17,19,21-tetrathiabicyclo[16.3.0]-henicos-1(15)-ene-17-thione (**2**) and 4-methylthio-5-(2-cyanoeth-

(8) Liu, W.; Wang, R.; Zhou, X. H.; Zuo, J. L.; You, X. Z. *Organometallics* **2008**, *27*, 126.

(9) Hansen, T. K.; Jørgensen, T.; Stein, P. C.; Becher, J. *J. Org. Chem.* **1992**, *57*, 6403.

(10) (a) Le Derf, F.; Mazari, M.; Mercier, N.; Levillain, E.; Trippé, G.; Riou, A.; Richomme, P.; Becher, J.; Garín, J.; Orduna, J.; Gallego-Planas, N.; Gorgues, A.; Sallé, M. *Chem.−Eur. J.* **2001**, *7*, 447. (b) Moore, A. J.; Goldenberg, L. M.; Bryce, M. R.; Petty, M. C.; Monkman, A. P.; Marenco, C.; Yarwood, J.; Joyce, M. J.; Port, S. N. *Adv. Mater.* **1998**, *10*, 395. (c) Lyskawa, J.; Le Derf, F.; Levillain, E.; Mazari, M.; Mazari, Sallé, M.; Dubois, L.; Viel, P.; Viel; Bureau, C.; Palacin, S. *J. Am. Chem. Soc.* **2004**, *126*, 12194.

(11) (a) Sans, M. Q.; Belser, P. *Coord. Chem. Rev.* **2002**, *229*, 59. (b) MacQueen, D. B.; Eyler, J. R.; Schanze, K. S. *J. Am. Chem. Soc.* **1992**, *114*, 1897.

(12) Simonsen, K. B.; Svenstrup, N.; Lau, J.; Simonsen, O.; Mørk, P.; Kristensen, G. J.; Becher, J. *Synthesis* **1996**, 407.

(13) Frisch, M. J.; Trucks, G. W.; Schlegel, H. B.; Scuseria, G. E.; Robb, M. A.; Cheeseman, J. R.; Montgomery, J. A., Jr.; Vreven, T.; Kudin, K. N.; Burant, J. C.; Millam, J. M.; Iyengar, S. S.; Tomasi, J.; Barone, V.; Mennucci, B.; Cossi, M.; Scalmani, G.; Rega, N.; Petersson, G. A.; Nakatsuji, H.; Hada, M.; Ehara, M.; Toyota, K.; Fukuda, R.; Hasegawa, J.; Ishida, M.; Nakajima, T.; Honda, Y.; Kitao, O.; Nakai, H.; Klene, M.; Li, X.; Knox, J. E.; Hratchian, H. P.; Cross, J. B.; Bakken, V.; Adamo, C.; Jaramillo, J.; Gomperts, R.; Stratmann, R. E.; Yazyev, O.; Austin, A. J.; Cammi, R.; Pomelli, C.; Ochterski, J. W.; Ayala, P. Y.; Morokuma, K.; Voth, G. A.; Salvador, P.; Dannenberg, J. J.; Zakrzewski, V. G.; Dapprich, S.; Daniels, A. D.; Strain, M. C.; Farkas, O.; Malick, D. K.; Rabuck, A. D.; Raghavachari, K.; Foresman, J. B.; Ortiz, J. V.; Cui, Q.; Baboul, A. G.; Clifford, S.; Cioslowski, J.; Stefanov, B. B.; Liu, G.; Liashenko, A.; Piskorz, P.; Komaromi, I.; Martin, R. L.; Fox, D. J.; Keith, T.; Al-Laham, M. A.; Peng, C. Y.; Nanayakkara, A.; Challacombe, M.; Gill, P. M. W.; Johnson, B.; Chen, W.; Wong, M. W.; Gonzalez, C.; Pople, J. A. *Gaussian 03*, revision B.04; Gaussian, Inc: Wallingford, CT, 2004.

Table 1. Crystallographic Data for Compounds 3, 4, and 8

	3	**4**·$CHCl_3$	**8**·$CHCl_3$·H_2O
empirical formula	$C_{24}H_{28}N_2O_4S_4$	$C_{28}H_{29}Cl_4N_2O_7ReS_4$	$C_{35}H_{27}BrCl_3N_2O_5ReS_4$
M_r	536.72	961.77	1056.29
cryst syst	monoclinic	triclinic	monoclinic
space group	$P2_1/c$	$P\bar{1}$	$C2/c$
a (Å)	24.396(7)	8.684(3)	22.257(16)
b (Å)	10.121(3)	13.561(5)	13.580(10)
c (Å)	10.180(3)	16.668(6)	26.61(2)
α (deg)	90.00	112.251(5)	90.00
β (deg)	96.305(5)	104.201(5)	95.969(15)
γ (deg)	90.00	91.120(5)	90.00
V (Å^3)	2498.3(12)	1747.3(11)	8000(10)
Z	4	2	8
ρ_c (g cm^{-3})	1.427	1.828	1.754
F(000)	1128	948	4128
T/K	293(2)	293(2)	293(2)
μ(Mo Kα)/mm^{-1}	0.415	4.069	4.488
index ranges	$-30 \le h \le 31$	$-10 \le h \le 9$	$-27 \le h \le 27$
	$-13 \le k \le 5$	$-16 \le k \le 8$	$-16 \le k \le 16$
	$-13 \le l \le 12$	$-19 \le l \le 19$	$-32 \le l \le 32$
GOF (F^2)	0.949	0.798	1.044
R_1[a], wR_2[b] ($I > 2\sigma(I)$)	0.0771, 0.1449	0.0743, 0.1315	0.0442, 0.0895
R_1[a], wR_2[b] (all data)	0.1848, 0.1789	0.1730, 0.1576	0.0609, 0.0925

[a] $R_1 = \sum||C| - |F_c||/\sum F_o|$. [b] $wR_2 = [\sum w(F_o^2 - F_c^2)^2/\sum w(F_o^2)]^{1/2}$.

Table 2. Selected Bond Lengths (Å) and Angles (deg) for 3

S(1)−C(14)	1.745(5)	S(1)−C(12)	1.753(4)
C(6)−C(12)	1.339(6)	C(13)−C(14)	1.326(5)
C(14)−S(1)−C(12)	95.7(2)	C(7)−C(6)−C(5)	118.9(4)
S(2)−C(12)−S(1)	112.8(2)	C(13)−S(3)−C(24)	100.9(2)
C(14)−S(4)−C(15)	102.6(2)		

ylthio)-1,3-dithiole-2-thione (**5**) were synthesized as described in the literature.[9,12] All solvents and chemicals were purchased from commercial sources and used as received.

4,5-Dithia-(3′,6′,9′,12′-tetraoxatetradecyl)-2-bis(2-pyridyl)-methylene-1,3-dithiole (3, BPyDT(O_4S_2)). Under a nitrogen atmosphere, a mixture of **1** (110 mg, 0.6 mmol) and **2** (214 mg, 0.6 mmol) was dissolved in 5 mL of toluene. After addition of 5 mL of $P(OEt)_3$, the reaction mixture was refluxed at 110 °C for 4 h. Then the solution was cooled to −20 °C, and an orange-red crude product was obtained. After separation by column chromatography on silica gel, an orange crystalline precipitate, **3**, was obtained. Yield: 141 mg (44%). Mp: 86−87 °C. IR (KBr, cm^{-1}): 2869, 1618, 1462, 1347, 1292, 1116. ^{1}H NMR (500 MHz, $CDCl_3$, ppm): δ 8.75 (d, 2H, J = 4.5, $BPyH^{6,6'}$), 7.68 (t, 2H, J = 6.8, $BPyH^{4,4'}$), 7.18 (t, 2H, J = 6.0, $BPyH^{3,3'}$), 7.11 (d, 2H, J = 7.5, $BPyH^{5,5'}$), 3.67−3.74 (m, 16H, $-SCH_2CH_2O-$ and $-OCH_2CH_2O-$), 3.06 (t, 4H, J = 6.3, $-SCH_2CH_2O-$). MS (MALDI-TOF): m/z 536.2 $[M]^+$. Anal. Calcd for $C_{24}H_{28}N_2O_4S_4$: C, 53.69; H, 5.23; N, 5.22. Found: C, 53.81; H, 5.12; N, 5.30.

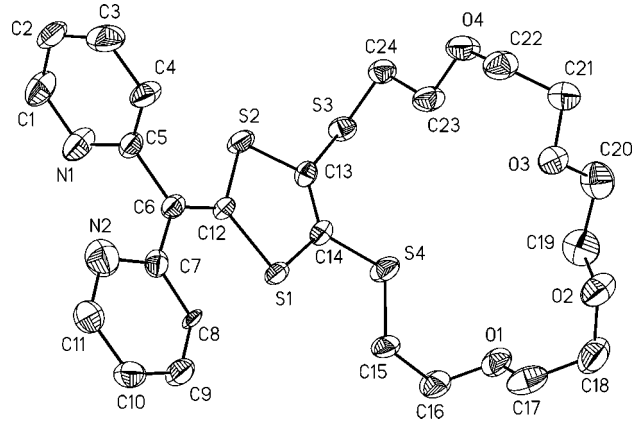

Figure 1. ORTEP view of compound **3** with the atom-numbering scheme. Hydrogen atoms are omitted for clarity. Ellipsoids are drawn at the 30% probability level.

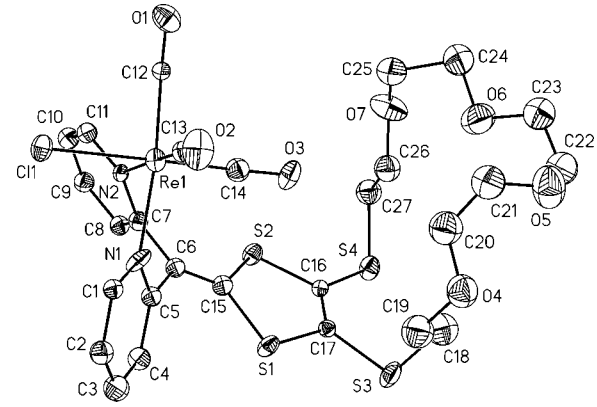

Figure 2. ORTEP view of complex **4** with the atom-numbering scheme. Hydrogen atoms are omitted for clarity. Ellipsoids are drawn at the 30% probability level.

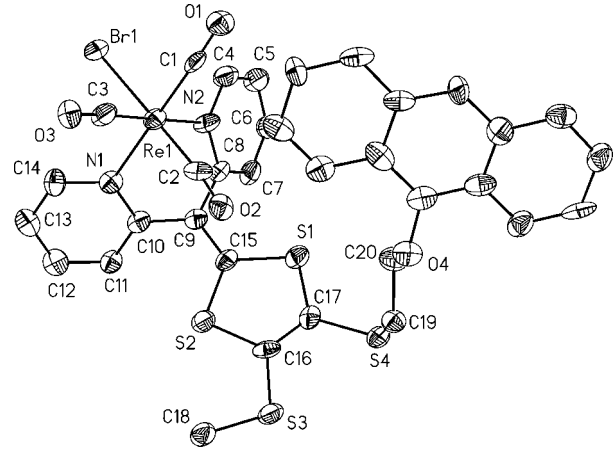

Figure 3. ORTEP view of complex **8** with the atom-numbering scheme. Hydrogen atoms are omitted for clarity. Ellipsoids are drawn at the 30% probability level.

ClRe(CO)$_3$(BPyDT(O_4S_2)) (4). Under a nitrogen atmosphere, a mixture of $Re(CO)_5Cl$ (36 mg, 0.1 mmol) and **3** (54 mg, 0.1

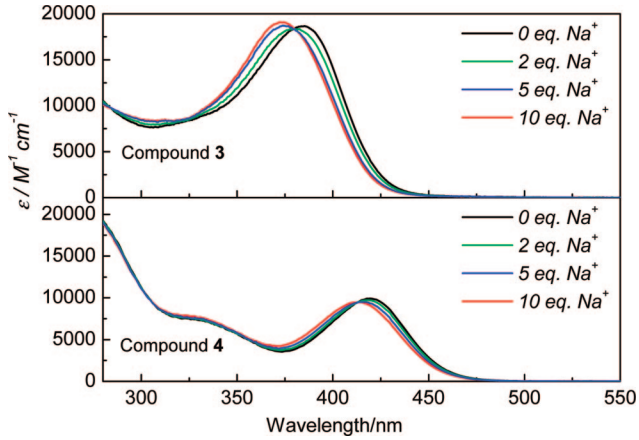

Figure 4. UV−vis absorption spectra of compounds **3** and **4**, on the addition of Na^+ in CH_2Cl_2/CH_3CN (v/v, 1:1).

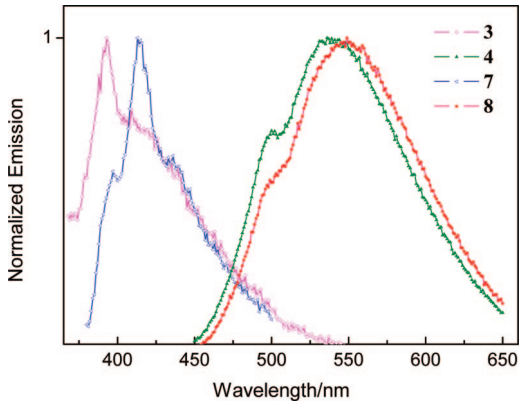

Figure 5. Normalized emission spectra of **3**, **4**, **7**, and **8** in CH_2Cl_2/CH_3CN (v/v, 9:1) at 298 K.

Table 3. Selected Bond Lengths (Å) and Angles (deg) for 4

Re(1)−N(1)	2.178(12)	Re(1)−N(2)	2.197(12)
Re(1)−C(12)	1.920(15)	Re(1)−C(13)	1.913(17)
Re(1)−C(14)	1.878(19)	Re(1)−Cl(1)	2.472(4)
S(1)−C(17)	1.746(14)	S(1)−C(15)	1.797(15)
C(6)−C(15)	1.292(19)	C(16)−C(17)	1.290(16)
N(1)−Re(1)−N(2)	82.4(4)	C(12)−Re(1)−N(1)	174.0(6)
C(13)−Re(1)−N(2)	175.6(6)	C(14)−Re(1)−Cl(1)	175.5(5)
C(5)−N(1)−Re(1)	122.3(9)	C(7)−N(2)−Re(1)	119.9(10)
C(5)−C(6)−C(7)	115.8(14)	S(2)−C(15)−S(1)	110.5(9)
C(17)−S(1)−C(15)	95.6(7)	C(16)−S(2)−C(15)	96.3(7)
C(17)−S(3)−C(18)	102.1(8)	C(16)−S(4)−C(27)	102.9(8)

mmol) was refluxed in 7 mL of toluene for 40 min. The solvent was removed to obtain the crude product. The pure yellow solid was obtained after chromatography by using CH_2Cl_2 as eluent (alumina). Yellow crystals were obtained from slow diffusion of Et_2O into a solution of **4** in $CHCl_3$. Yield: 71 mg (84%). Mp: >280 °C. IR (KBr, cm^{-1}): 2018, 1906, 1885 ($\nu_{C\equiv O}$). ^1H NMR (500 MHz, $CDCl_3$, ppm): δ 9.13 (d, 2H, J = 5.3, $BPyH^{6,6'}$), 7.89 (t, 2H, J = 7.3, $BPyH^{4,4'}$), 7.71(d, 2H, J = 7.7, $BPyH^{3,3'}$), 7.37 (t, 2H, J = 6.5, $BPyH^{5,5'}$), 3.61−3.76 (m, 16H, $-SCH_2CH_2O-$ and $-OCH_2CH_2O-$), 2.96−3.08 (m, 4H, $-SCH_2CH_2O-$). MS (MALDI-TOF): m/z 807.2 $[M - Cl]^+$. Anal. Calcd for $C_{28}H_{29}Cl_4N_2O_7ReS_4$: C, 34.96; H, 3.04; N, 2.91. Found: C, 34.87; H, 3.12; N, 2.82.

4-Methylthio-5-(2-cyanoethylthio)-2-bis(2-pyridyl)methylene-1,3-dithiole (6, BPyDT(SMe)(SCH_2CH_2CN)). The ligand precursor **6** was synthesized from **1** and **5** under the same conditions as described above for **3**. It was isolated as a yellow solid in 41% yield. IR (KBr, cm^{-1}): 2245 ($\nu_{C\equiv N}$). ^1H NMR (500 MHz, $CDCl_3$, ppm): δ 8.78 (t, 2H, J = 4.5, $BPyH^{6,6'}$), 7.67−7.71 (m, 2H, $BPyH^{4,4'}$), 7.18−7.23 (m, 2H, $BPyH^{3,3'}$), 7.16 (d, 1H, J = 8.0, $BPyH^5$), 7.10 (d, 1H, J = 8.0, $BPyH^{5'}$), 3.06 (t, 2H, J = 7.3, $-SCH_2CH_2CN$), 2.71 (t, 2H, J = 7.3, $-SCH_2CH_2CN$), 2.49 (s, 3H, $-SCH_3$). MS (ESI): m/z 400.6 $[M]^+$. Anal. Calcd for $C_{18}H_{15}N_3S_4$: C, 53.83; H, 3.76; N, 10.46. Found: C, 53.74; H, 3.69; N, 10.37.

Table 4. Selected Bond Lengths (Å) and Angles (deg) for 8

N(1)−Re(1)	2.168(4)	N(2)−Re(1)	2.172(5)
C(1)−Re(1)	1.869(6)	C(2)−Re(1)	1.876(6)
C(3)−Re(1)	1.875(5)	Br(1)−Re(1)	2.6150(18)
C(9)−C(15)	1.331(6)	C(15)−S(1)	1.759(5)
C(17)−S(1)	1.693(5)	C(16)−C(17)	1.364(7)
N(1)−Re(1vN(2)	82.99(17)	C(2)−Re(1)−Br(1)	179.56(17)
C(1)−Re(1)−N(1)	177.39(19)	C(3)−Re(1)−N(2)	176.7(2)
C(18)−S(3)−C(16)	104.2(3)	C(17)−S(4)−C(19)	103.3(2)

4-Methylthio-5-[{2-(9′-anthryloxy)ethyl}thio]-2-bis(2-pyridyl)-methylene-1,3-dithiole (7, BPyDT(SMe)(SEA)). Under a nitrogen atmosphere, to a solution of **6** (201 mg, 0.5 mmol) in THF (15 mL) was added a solution of $CsOH\cdot H_2O$ (84 mg, 0.5 mmol) in methanol (5 mL) over a period of 10 min. The mixture was stirred for an additional 30 min, and a solution of 9-(2-bromoethoxyl)-anthracene (151 mg, 0.5 mmol) in CH_2Cl_2 (15 mL) was added. The reaction mixture was further stirred overnight at room temperature. The resulting mixture was concentrated, dissolved in CH_2Cl_2, and washed with water. Purification by column chromatography (CH_2Cl_2) on silica gel gave **7** as an orange-red oil in 56% yield. IR (KBr, cm^{-1}): 2361, 1581, 1457, 1423, 1337, 1277, 1089, 736; ^1H NMR (500 MHz, $CDCl_3$, ppm): δ 8.78 (d, 1H, J = 3.9, $BPyH^6$), 8.73 (d, 1H, J = 4.0, $BPyH^{6'}$), 8.37 (t, 2H, $anthrylH^{1,8}$); 8.25 (s, 1H, $anthrylH^{10}$), 8.01 (t, 2H, J = 5.4, $anthrylH^{4,5}$), 7.67−7.70 (m, 2H, $anthrylH^{3,6}$), 7.48 (t, 4H, J = 4.4, $anthrylH^{2,7}$ and $BPyH^{4,4'}$), 7.09−7.19 (m, 4H, $BPyH^{3,3',5,5'}$), 4.45 (t, 2H, J = 6.4, $-SCH_2CH_2CN$), 3.48 (t, 2H, J = 6.4, $-SCH_2CH_2CN$), 2.48 (t, 3H, J = 11.2, $-SCH_3$). MS (MALDI-TOF): m/z 568.1 $[M]^+$. Anal. Calcd for $C_{31}H_{24}N_2OS_4$: C, 65.46; H, 4.25; N, 4.93. Found: C, 65.37; H, 4.26; N, 4.90.

$BrRe(CO)_3$(BPyDT(SMe)(SEA)) (8). Under a nitrogen atmosphere, a mixture of $Re(CO)_5Br$ (43 mg, 0.12 mmol) and **7** (68 mg, 0.12 mmol) was refluxed in 8 mL of toluene for 1.5 h. The solvent was removed to obtain the crude product. Orange, solid **8** was obtained after chromatography on alumina by using CH_2Cl_2 as eluent. Orange crystals were obtained from $CHCl_3/Et_2O$. Yield: 90 mg (82%). Mp: 142−143 °C. IR (KBr, cm^{-1}): 2017, 1918, 1892 ($\nu_{C\equiv O}$). ^1H NMR (500 MHz, $CDCl_3$, ppm): δ 9.25 (d, 2H, J = 6.6, $BPyH^{6,6'}$), 8.27−8.33 (m, 2H, $anthrylH^{1,8}$), 7.70−8.03 (m, 9H, $anthrylH^{2-7,10}$ and $BPyH^{4,4'}$), 7.33−7.50 (m, 4H, $BPyH^{3,3',5,5'}$), 4.40 (t, 2H, J = 5.0, $-SCH_2CH_2CN$), 3.38−3.42 (m, 2H, $-SCH_2CH_2CN$), 2.40−2.45 (m, 3H, $-SCH_3$). MS (MALDI-TOF): m/z 839.1 $[M - Br]^+$. Anal. Calcd for $C_{35}H_{27}BrCl_3N_2O_5ReS_4$: C, 39.80; H, 2.58; N, 2.65. Found: C, 39.69; H, 2.67; N, 2.56.

Crystal Structure Determination. The data were collected on a Bruker Smart Apex CCD diffractometer equipped with graphite-monochromated Mo Kα (λ = 0.71073 Å) radiation using a $\omega-2\theta$ scan mode at 293 K. The highly redundant data sets were reduced using SAINT and corrected for Lorentz and polarization effects. Absorption corrections were applied using SADABS supplied by Bruker. The structure was solved by direct methods and refined by full-matrix least-squares methods on F^2 using SHELXTL-97. All non-hydrogen atoms were found in alternating difference Fourier syntheses and least-squares refinement cycles and, during the final cycles, refined anisotropically. Hydrogen atoms were placed in calculated positions and refined as riding atoms with a uniform value of U_{iso}.

Computational Details. All calculations were carried out with Gaussian03 programs.[13] We employed the density functional theory (DFT) and time-dependent DFT (TDDFT) with no symmetry constraints to investigate the optimized geometries, HOMOs, and LUMOs with the three-parameter hybrid functional (B3LYP).[14] The

Table 5. Electronic Absorption and Luminescence Data for Compounds 3, 4, 7, and 8 in CH_2Cl_2 Solution at 298 K

	absorption	luminescence	
compound	λ_{abs}/nm (ε/M^{-1} cm^{-1})	λ_{ex}/nm	λ_{em}/nm
3	258 (15 448), 385 (18 700)	353	393
4	266 (21 500), 325 sh (7500), 420 (9900)	436	539
7	256 (28 000), 273 (17 900), 349 (2200), 369 (2100), 389 (1800)	368	413
8	256 (70 500), 270 sh (30 900), 348 (6400), 369 (5900), 390 (6300), 416 (6600)	439	549

B3LYP calculations were carried out by the 6-31G* basis set for C, H, O, Cl, Br, and S atoms and the effective core potentials (ECP) such as LANL2DZ for Re atoms.

Results and Discussions

Synthesis and Characterization. The ligand precursor **2** was prepared by a previously reported route, using the important high-dilution method to improve the yield. The ligand **3** was prepared by the cross-coupling method in the presence of $P(OEt)_3$ and purified through column chromatography. Then reaction of $Re(CO)_5Cl$ with ligand **3** in refluxing toluene afforded the complex **4** with high yield (Scheme 1).

The ligand precursor **6** was also prepared via $P(OEt)_3$-mediated cross-coupling reaction. After deprotecting the cyanoethyl group with 1 equiv of $CsOH \cdot H_2O$, the subsequent reaction between the monoanions and 9-(2-bromoethoxy)anthracene gave the ligand **7**. Complex **8** was obtained by the treatment of **7** with $Re(CO)_5Br$ followed by purification on alumina (Scheme 2).

All compounds are soluble in most organic solvents and air stable in both fluid solution and the solid state. Characterization of all new compounds has been accomplished by mp, IR, ^1H NMR, UV−vis, and mass spectrometry. ^1H NMR spectra for **3** and **4** display four resonances at δ 8.75/9.13, 7.68/7.89, 7.18/7.71, and 7.11/7.37, respectively, of the protons on the two pyridine rings. Compared with **3**, the proton signals on the pyridine rings in complex **4** are shifted to low-field since the formation of coordination bonds influenced the electronic distribution. The resonances of protons in the crown cycles for **3** and **4** are almost at the same position, which are in good agreement with their structures. The peaks for protons on the pyridine and anthryl groups for **7** and **8** are overlapped, and therefore it is difficult to make a clear assignment for them.

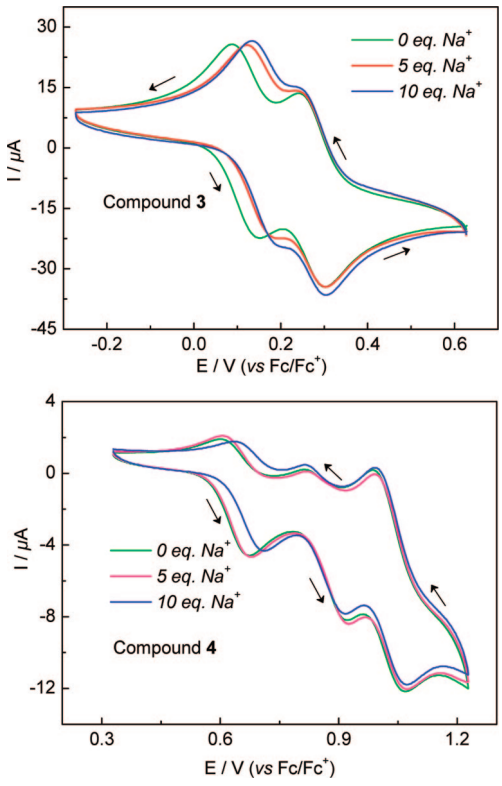

Figure 6. Cyclic voltammogram of compounds **3** (top) and **4** (bottom) (5×10^{-4} M) upon addition of Na^+, measured in CH_3CN/CH_2Cl_2 (1:1) (vs Fc/Fc^+), at a scan rate of 100 mV/s.

Crystal Structure Description. The solid structures of compounds **3**, **4**, and **8** were determined by single-crystal X-ray diffraction. Crystallographic data are shown in Table 1, and selected bond lengths and angles are listed in Tables 2−4.

Figure 1 gives the ORTEP view of **3** with atomic numbering. The macrocycle part of ligand **3** adopts a crown conformation, which is in favor of metal complexation, like some other monocrown compounds. The O_4S_2 crown ether group is bent toward one side of the five-membered 1,3-dithiole ring (C12, S1, C14, C13, and S2). The 1,3-dithiole ring, one carbon atom (C6), two sulfur atoms (S3 and S4) from the macrocycle, and one pyridine group (N2, C7, C8, C9, C10, and C11) are in one plane. It is almost vertical to the other pyridine ring with a dihedral angle of 88.7°.

The molecular structure of complex **4** is shown in Figure 2. In the molecule, the rhenium atom is in a distorted octahedral coordination environment with three carbonyl ligands in a *fac* arrangement, two N atoms from two pyridine rings of the new bispyridine ligand, and a chlorine atom. The bond lengths and angles around the rhenium(I) center are in normal ranges, as observed in similar rhenium(I) tricarbonyl complexes with other polypyridine ligands.[15] Owing to the steric effect from the chelating bis(2-pyridyl) group, a N−Re−N angle of less than 90° is observed (82.4(4)°). Different from the structure in **3**, the molecule of complex **4** adopts a saddle-like configuration: S1, S2, C16, C17, S3, and S4 are coplanar, while two pyridine rings both deviate from this plane, and the crown ether part is tilted in the parallel direction.

Complex **8** crystallizes in the monoclinic space group *C*2/*c* with one solvated $CHCl_3$ and one solvated H_2O molecule (Figure 3). Similar to **4**, an essentially pseudo-octahedral geometry about the rhenium atom with the usual *fac* arrangement of the three carbonyl groups was observed. Correspondingly, the bite angle of N(1)−Re(1)−N(2) is 82.9 (9)°.

Electronic Absorption and Luminescence Properties. The UV−vis absorption spectra of compounds **3** and **4** are shown

(14) (a) Lee, C.; Yang, W.; Parr, R. G. *Phys. Rev. B* **1988**, *37*, 785. (b) Miehlich, B.; Savin, A.; Stoll, H.; Preuss, H. *Chem. Phys. Lett.* **1989**, *157*, 200.

(15) (a) Grewea, J.; Hagenbacha, A.; Stromburga, B.; Albertob, R.; Vazquez-Lopezc, E.; Abram, U. *Z. Anorg. Allg. Chem.* **2003**, *629*, 303. (b) Moya, S. A.; Guerrero, J.; Pastene, R.; Schmidt, R.; Sariego, R.; Sartori, R.; Sanz-Aparicio, J.; Fonseca, I.; Martinez-Ripoll, M. *Inorg. Chem.* **1994**, *33*, 2341. (c) Coe, B. J.; Curati, N. R. M.; Fitzgerald, E. C.; Coles, S. J.; Horton, P. N.; Light, M. E.; Hursthouse, M. B. *Organometallics* **2007**, *26*, 2318. (d) Kirgan, R.; Simpson, M.; Moore, C.; Day, J.; Bui, L.; Tanner, C.; Rillema, D. P. *Inorg. Chem.* **2007**, *46*, 6464.

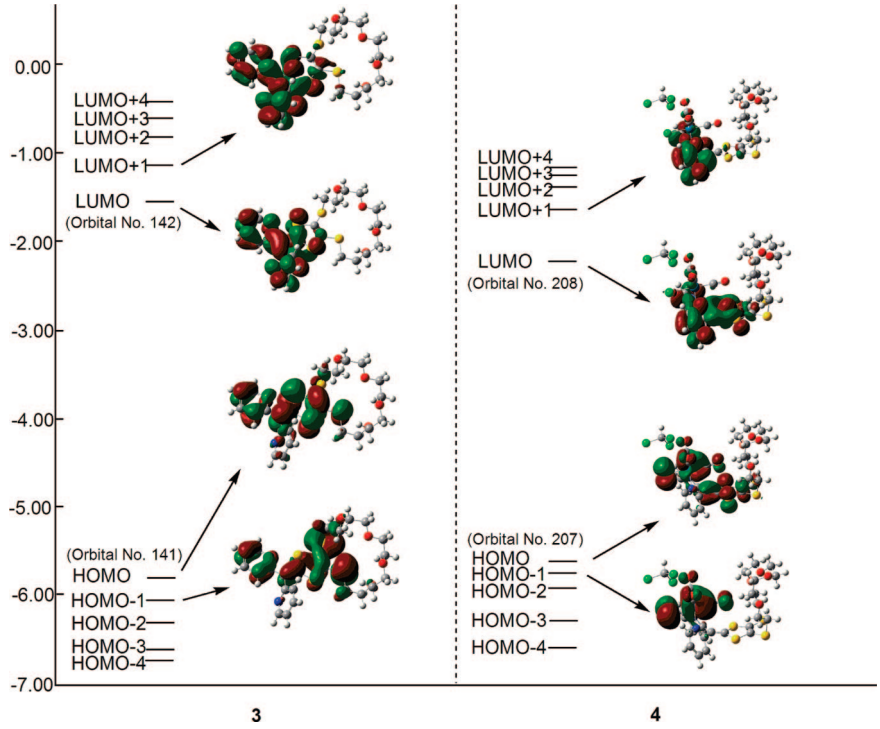

Figure 7. Molecular orbital energy diagrams and graphical representation for frontier orbitals of compounds **3** and **4**.

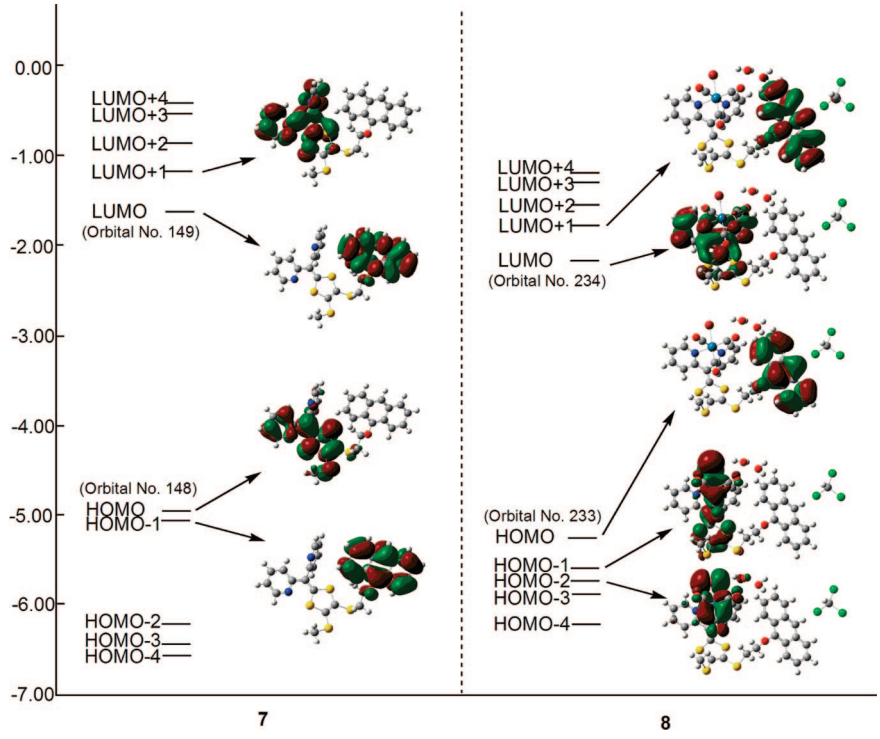

Figure 8. Molecular orbital energy diagrams and graphical representation for frontier orbitals of **7** and **8**.

in Figure 4. The high-energy absorption peaks (258 and 385 nm) for ligand **3** can be assigned to the $\pi-\pi^*$ transition. Similarly, spin-allowed intraligand (IL, $\pi-\pi^*$) transitions (the absorption peak at 266 nm and the shoulder at ca. 325 nm) for complex **4** were observed. With reference to previous studies on related rhenium(I) systems,[8,15c,d] the absorption band at 420 nm for **4** is attributed to the $d\pi(Re)-\pi^*$(ligand) transition. Hypsochromic shifts of the absorption peaks have been observed after addition of Na^+ to the solutions of **3** and **4**. The 1:1 complexation model for metal ion binding was supported by the good agreement of the experimental data with the theoretical fit (Figures S1 and S2). These shifts (about 9−13 nm) suggest that the complexation between the alkali metal ions and the crown segments induces changing of conjugation in the whole system and increases the |HOMO−LUMO| gap.[16] The log K_a values of **3** and **4** for Na^+ ions were found to be 3.05 ± 0.11 and 2.61 ± 0.03, respectively (calculated through nonlinear least-squares fitting).[6b,17]

Figure S3 shows the absorption spectra of **7** and **8**. In addition to the intense absorptions at ca. 240−320 nm, which are the

Table 6. Main Experimental and Calculated Optical Transitions for 3, 4, 7, and 8

compound	orbital excitations	character	calcd/nm	f [a]	exptl/nm
3	HOMO→LUMO	$\pi\rightarrow\pi^*$	391	0.0858	385, 285
	HOMO→LUMO+1	$\pi\rightarrow\pi^*$	391	0.2609	
	HOMO→LUMO+2	$\pi\rightarrow\pi^*$	338	0.0463	
	HOMO−1→LUMO	$\pi\rightarrow\pi^*$	277	0.0355	
4	HOMO→LUMO	MLCT	449	0.0263	420, 325
	HOMO−1→LUMO	MLCT	445	0.0035	
	HOMO−2→LUMO	MLCT	408	0.1177	
	HOMO→LUMO+1	$\pi\rightarrow\pi^*$	369	0.0077	
	HOMO→LUMO+2	$\pi\rightarrow\pi^*$	350	0.0520	
7	HOMO→LUMO	ICT	413	0.0043	389, 369, 349
	HOMO−1→LUMO	$\pi\rightarrow\pi^*$	391	0.0935	
	HOMO→LUMO+1	$\pi\rightarrow\pi^*$	385	0.1080	
	HOMO→LUMO+2	$\pi\rightarrow\pi^*$	355	0.2019	
	HOMO−1→LUMO+1	ICT	351	0.0142	
8	HOMO-1→LUMO	MLCT	452	0.0177	416, 390, 369
	HOMO−2→LUMO	MLCT	442	0.0036	
	HOMO→LUMO+1	$\pi\rightarrow\pi^*$	396	0.1136	
	HOMO→LUMO+2	$\pi\rightarrow\pi^*$	369	0.0144	

[a] Oscillator strength.

typical $\pi-\pi^*$ transitions, three relatively weak peaks (around 350, 370, and 390 nm) inherent for an anthryl group have been observed. Being a tricarbonyl rhenium(I) bispyridine complex, compound **8** also exhibits an absorption peak at 416 nm resulting from the charge transfer between rhenium and the ligand.

The normalized emission spectra of compounds **3**, **4**, **7**, and **8** in CH_2Cl_2/CH_3CN (v/v, 9:1) at 298 K are shown in Figure 5, and their spectral data are given in Table 5. Compound **3** displays blue luminescence derived from $\pi^*-\pi$ relaxation. Owing to the luminophore anthryl group, the emission of **7** moves to the lower energy region. Upon photoexcitation, compounds **4** and **8** exhibit intense, greenish-yellow luminescence in fluid solutions under ambient conditions, which are characteristic of MLCT (metal-to-ligand charge transfer) emissions of rhenium(I) complexes. No obvious emission change is observed when Na^+ or other alkali cations are added to the solutions of compounds **3** and **4**.

Electrochemistry. The cation-binding properties of compounds **3** and **4** have also been investigated by cyclic voltammetry (CV) in CH_3CN/CH_2Cl_2 (v/v, 1:1) in the presence of Na^+ (Figure 6). The CV of **3** exhibits two reversible one-electron oxidation processes to the radical cation and the dication with $E^1_{1/2} = 0.120$ V and $E^2_{1/2} = 0.273$ V. After the addition of $NaClO_4$ to the solution, the first half-wave potential ($E^1_{1/2}$) shifted positively, while $E^2_{1/2}$ remained unchanged, indicating that the electrostatistic expulsion of the added metal cation from the doubly oxidized compound takes place at the second potential.[9] The largest shift ($\Delta E = 48$ mV) of $E^1_{1/2}$ was obtained when 10 equiv of Na^+ was added. No obvious response was observed when other alkali cations such as Li^+ and K^+ were added to the system.

The CV of **4** exhibits three reversible one-electron oxidation processes with $E^1_{1/2} = 0.639$ V, $E^2_{1/2} = 0.864$ V, and $E^3_{1/2} = 1.037$ V. The first and second redox couples may be assigned to redox processes (**4**/**4**$^+$, **4**$^+$/**4**$^{2+}$), and the third one is associated with the rhenium(I)-based oxidation−reduction (Re^I/Re^{II}).[15,18] The addition of $NaClO_4$ also resulted in a gradual positive shift of the first half-wave potential, whereas the second one remained unchanged. The maximum shift ($\Delta E_1 = 35$ mV) was reached in the presence of 10 equiv of Na^+. It has no response to other alkali cations Li^+ and K^+. The good electrochemical response and selectivity reveal that both **3** and **4** could be novel redox-active sensors.

The cyclic voltammograms of compounds **7** and **8** are shown in Figures S4 and S5. For complex **8**, it displays three quasi-reversible redox potentials ($E^1_{1/2} = 0.695$ V, $E^2_{1/2} = 0.915$ V, and $E^3_{1/2} = 1.095$ V). As we all know, both electronic and structural factors from functional groups attached to the core framework will affect the resulting electrochemical properties. Compared with **4**, complex **8** has higher redox potentials. This indicates that the crown ether segment in **4** contributes to larger delocalization of the molecule than the anthryl group in **8** and consequently makes it easier to oxidize.

Computational Studies. All calculations on compounds **3**, **4**, **7**, and **8** were carried out by using density functional theory (DFT) and time-dependent DFT (TDDFT). Figures 7 and 8 show the plots of the most representative molecular frontier orbitals for **3**, **4**, **7**, and **8**. Other relevant frontier orbitals are available in the Supporting Information. Table 6 summarizes the spin-allowed electronic transitions calculated with the TDDFT method. For all the compounds, the calculated transitions agree with the experimental ones.

The HOMO−1, HOMO, LUMO, LUMO+1, and LUMO+2 orbitals of molecule **3** all predominately delocalize on the $BPyDTS_2$ moiety, with the crown ether moiety almost empty. Thus, the UV−vis absorption bands at 385 and 285 nm are of $\pi\rightarrow\pi^*$ character, probably with some mixing of a charge transfer character from the 1,3-dithiole five-membered ring to the pyridyl group.

According to DFT and TDDFT calculations, the lowest energy band experimentally found for complex **4** around 420 nm mainly originates from HOMO→LUMO, HOMO−1→LUMO, and HOMO−2→LUMO transitions, which can be assigned to MLCT due to the orbital characters of the corresponding starting and arriving states (see Supporting Information). This type of MLCT transition is similar to those observed for tricarbonyl rhenium(I) complexes containing bidendate polypyridyl ligands.[15d,19] In the UV−vis spectra, the absorption shoulder at 325 nm may come from the HOMO→LUMO+1 and HOMO→LUMO+2 transitions ($\pi\rightarrow\pi^*$).

For compound **7**, the characteristic $BPyDTS_2$ of the HOMO and anthryl groups characteristic of the LUMO indicate that the HOMO→LUMO absorption transition possesses an intramolecular charge transfer (ICT) character, while the HOMO→LUMO+1 and HOMO→LUMO+2 transitions are mainly on $BPyDTS_2$, which suggests such transitions are of a $\pi\rightarrow\pi^*$ character. Similarly, the HOMO−1→LUMO transition dominantly on the anthryl group also suggests a $\pi\rightarrow\pi^*$ character. The experimental absorption band for complex **8** at 416 nm is of MLCT character, relevant to the calculated bands at 452 and 442 nm, coming from a mixed transition of HOMO−1→LUMO and HOMO−2→LUMO. The orbitals of HOMO and LUMO+1 are nearly completely delocalized on the anthryl group; thus, the absorption band at 390 nm is of $\pi\rightarrow\pi^*$ character. The experimentally obtained band at 369 nm belongs to an ICT transition, originating from the HOMO to LUMO+2 transition calculated at 369 nm. Moreover, the electrons in **8** are less delocalized than those in **4**, which could

(16) Jousselme, B.; Blanchard, P.; Levillain, E.; Delaunay, J.; Allain, M.; Richomme, P.; Rondeau, D.; Gallego-Planas, N.; Roncali, J. *J. Am. Chem. Soc.* **2003**, *125*, 1363.

(17) Tang, W. S.; Lu, X. X.; Wong, K. M. C.; Yam, V. W. W. *J. Mater. Chem.* **2005**, *15*, 2714.

(18) (a) Lin, R.; Fu, Y.; Brock, C. P.; Guarr, T. F. *Inorg. Chem.* **1992**, *31*, 4346. (b) Si, Z.; Li, J.; Li, B.; Zhao, F.; Liu, S.; Li, W. *Inorg. Chem.* **2007**, *46*, 6155.

(19) (a) Machura, B.; Penczek, R.; Kruszynski, R. *Polyhedron* **2007**, *26*, 2470. (b) Dattelbaum, D. M.; Omberg, K. M.; Hay, P. J.; Gebhart, N. L.; Martin, R. L.; Schoonover, J. R.; Meyer, T. J. *J. Phys. Chem. A* **2004**, *108*, 3527.

further support the higher redox potentials observed in electrochemical studies.

In conclusion, two novel bispyridine ligands, one with crown ether-annelated 1,3-dithiole-2-ylidene (**3**) and the other with anthracene-extended 1,3-dithiole-2-ylidene (**7**), have been synthesized. Their respective tricarbonyl rhenium(I) complexes, **4** and **8**, have been prepared and thoroughly characterized. All four compounds are luminescent at room temperature. The results from electrochemical studies show that both compounds **3** and **4** are only responsive to Na^+ ions, with remarkable shifts of the first redox couples, and could be new sensors for Na^+ ions.

Acknowledgment. This work was supported by the Major State Basic Research Development Program (2006CB806104 and 2007CB925103), the National Science Fund for Distinguished Young Scholars of China (Grant 20725104), and the National Natural Science Foundation of China (Grant 20721002).

Supporting Information Available: Crystallographic data for compounds **3**, **4**, and **8** in CIF format; plot of UV−vis absorbance vs [Na^+] of compounds **3** and **4**, UV−vis absorption spectra of **7** and **8**; cyclic voltammogram of **7** and **8**; calculated electron distributions of **3**, **4**, **7**, and **8**; calculated excitation energies and oscillator strengths of compounds **3**, **4**, **7**, and **8**. This material is available free of charge via the Internet at http://pubs.acs.org.

OM800178K